

# The External Shear Acting on Gravitational Lens B 1422+231<sup>1</sup>

Tomislav Kundić<sup>2</sup>, David W. Hogg<sup>2</sup>, Roger D. Blandford<sup>2</sup>, Judith G. Cohen<sup>3</sup>, Lori M. Lubin<sup>4</sup> and James E. Larkin<sup>5</sup>

## ABSTRACT

In a number of multiply imaged quasar systems, a significant contribution to the lensing potential is provided by groups and clusters of galaxies associated with the primary lens. As part of an ongoing effort to gather observational data on these systems, we present spectroscopy and near-infrared and optical photometry of galaxies in the field of the quadruple lens system B 1422+231. The spectra show that the primary lens and five nearby galaxies belong to a compact group at  $z = 0.338$ . The median projected radius of this group is  $35 h^{-1}$  kpc and its velocity dispersion is  $\sim 550 \text{ km s}^{-1}$ . A straightforward application of the virial theorem yields a group mass of  $1.4 \times 10^{13} h^{-1} M_{\odot}$ , which provides sufficient external shear to produce the observed image configuration. This data rules out a class of models and improves the system's prospects for a measurement of the Hubble constant.

*Subject headings:* cosmology — distance scale — gravitational lensing — galaxies: clustering – quasars: individual (B 1422+231)

---

<sup>1</sup>Based on observations obtained at the W. M. Keck Observatory, which is operated jointly by the California Institute of Technology and the University of California

<sup>2</sup>Theoretical Astrophysics, California Institute of Technology, Mail Code 130-33, Pasadena, CA 91125; tomislav, hogg, rdb@tapir.caltech.edu

<sup>3</sup>Palomar Observatory, California Institute of Technology, Mail Code 105-24, Pasadena, CA 91125; jlc@astro.caltech.edu

<sup>4</sup>The Observatories of the Carnegie Institution of Washington, 813 Santa Barbara Street, Pasadena, CA 91101; lml@ociw.edu

<sup>5</sup>Palomar Observatory, California Institute of Technology, Mail Code 320-47, Pasadena, CA 91125; currently at the Department of Astronomy and Astrophysics, University of Chicago; larkin@agrabah.uchicago.edu

## 1. Introduction

One of the most exciting astrophysical applications of gravitational lensing is the determination of the cosmological distance scale. The technique of measuring the Hubble constant in multiply imaged variable sources was developed by Refsdal (1964), who realized that the time delay between variations of the individual images is inversely proportional to  $H_0$ . So far, two accurate time delays have been reported in the literature, one in the double quasar Q 0957+561 (Kundić et al. 1996) and the other in the quadruple quasar PG 1115+080 (Schechter et al. 1997), yielding consistent values of the Hubble constant. However, before Refsdal’s method is universally accepted as a competitor to the traditional distance ladder approach, it has to be applied to a statistically significant sample of systems with different image morphologies and source and lens redshifts to verify the validity of the lensing models (Blandford & Kundić 1997). One of the systems that shows good promise for extending the time delay work is the quadruple quasar B 1422+231.

The gravitational lens system B 1422+231 ( $V = 16.5$ ,  $z = 3.62$ ) was discovered by Patnaik et al. (1992a) as part of the JVAS radio survey (Patnaik et al. 1992b, 1994). VLA and MERLIN maps of the system exhibited four-image structure with three bright unresolved images (A, B and C) opposite a much fainter image D. The brighter components were shown to have similar polarization properties and spectral indices, strongly suggesting that they are lensed images of the same source. Infrared observations of the system (Lawrence et al. 1992) confirmed the relative positions and relative fluxes of the four images. The only disagreement between the radio and the optical data is in the flux ratio of images A and B. This is discussed in more detail in §4. Optical imaging of the system revealed the primary lens (Yee & Ellingson 1994) and five nearby galaxies (Remy et al. 1993, Bechtold & Yee 1995). A tentative redshift of the lensing galaxy was obtained by Hammer et al. (1995). Astrometry of the system with the Faint Object Camera on the Hubble Space Telescope (Impey et al. 1996) confirmed the radio positions of Patnaik et al. (1992a) with  $0.01''$  accuracy. FOS spectra of the four images were shown to be strikingly similar, providing additional evidence for the lensing origin of the system.

Because this system shows evidence for variability in visual luminosity (Hjorth et al. 1996, Yee & Bechtold 1996, Turner et al. 1997) and radio morphology (Patnaik, private communication), it offers a good prospect for measuring the Hubble constant. For this reason it is extremely important to constrain, as tightly as possible, the suite of acceptable lens models.

In this paper we present spectroscopy and visual and near-infrared imaging of the system with the goal of measuring the redshift of the main lensing galaxy and its five neighbors, and estimating the gravitational potential contributed by these galaxies based

on their mass-to-light ratios and the velocity dispersion of the group.

## 2. Observations

### 2.1. Optical and Near-Infrared Photometry

$R$  band images of the B 1422+231 field were taken on 1995 July 30 with the Low Resolution Imaging Spectrograph (LRIS; Oke et al. 1995) on the 10 m Keck telescope. The scale on the 2048x2048 LRIS detector is 0.215 arcsec/pixel. Exposures totaling 100 seconds were registered and combined to produce the final frame from which relative positions and magnitudes of galaxies in the field were measured. The FWHM of the point spread function in the combined image was  $0.75''$ . A  $2' \times 2'$  region of the frame is shown in Fig. 1. The central object in the image (marked B 1422+231) contains four quasar images and the main lensing galaxy G1. The remaining lens group galaxies (G2, G3, G4, G5 and G6) are located southeast of the quasar. Galaxy G7 was also detected in near-infrared images (see below), but its spectrum is not available. G8, G9 and G10 are emission line galaxies with redshifts  $z_8 = 0.2355$ ,  $z_9 = 0.4650$ , and  $z_{10} = 0.4555$ . They are unrelated to the lensing group (see below), but close enough to the line of sight to the source to be incorporated perturbatively into any detailed lens models. The positions of all galaxies relative to image B and their  $R$  magnitudes measured in a  $3''$  circular aperture are listed in Table 1. Since we were unable to determine accurately the position of image B, the coordinates of a nearby star (S1) are also given in the table. We estimate that the relative positional error is  $\lesssim 0.2''$ , and the error in relative magnitudes is  $\lesssim 0.2$  mag. The zero point of the  $R$  magnitude scale was determined by comparing our data with photometry of Remy et al. (1993).

Near-infrared  $J$ ,  $H$  and  $K_s$  images of the field were taken in March 1994 with the Near Infrared Camera (NIRC; Matthews & Soifer 1994) on the Keck telescope. The camera is equipped with a  $256 \times 256$  Santa Barbara Research Center InSb detector with a scale of 0.15 arcsec/pixel, resulting in a field of view of  $38.4'' \times 38.4''$ . The images were taken in a standard “box 9” pattern in which the telescope is moved roughly 5 arcsec between exposure in a regular  $3 \times 3$  grid. Bright objects in the frames are masked off and then the 9 images from each pattern are medianed together to produce a sky and flat field frame. Due to a significant time varying background, a twilight or dome flat does not provide adequate flat fielding. Exposures in each band were registered using bright objects in the field and were then averaged together to yield the final images. The total exposure times were 120 s in  $J$ , 200 s in  $H$ , and 400 s in  $K_s$  (Fig. 2). The FWHM of the point spread function was  $0.7''$  in the combined frames. The zero point of the magnitude scale was determined by repeated observations of 4 UKIRT faint standards (Casali & Hawarden 1992), yielding photometric

uncertainties of roughly 0.025 mag for each of the infrared bands. The resulting  $J$ ,  $H$  and  $K_s$  photometry of the lensing group galaxies is listed in Table 1. These magnitudes are quoted for a circular aperture with a  $3''$  diameter. Since the galaxies extend beyond this radius, an aperture correction was applied before performing mass-to-light ratio calculations in the following section. Unfortunately, group galaxy G5 was not covered by the NIRC field of view.

## 2.2. Spectroscopy

LRIS spectra of B 1422+231 were taken on 1995 July 30–31, 1997 March 2, and 1997 June 2. On the first observing run (July 1995), a 300 line  $\text{mm}^{-1}$  grating was used which provides spectral resolution of  $2.47 \text{ \AA}/\text{pixel}$ . The second and third set of spectra (March and June 1997) were taken with a higher-resolution 600 line/mm grating yielding  $1.25 \text{ \AA}/\text{pixel}$ . A  $1.0''$  slit was used throughout the observing program. The resulting FWHM of isolated sky lines was 10–15  $\text{\AA}$  in the low-resolution spectra and 4–5  $\text{\AA}$  in the high-resolution spectra. Detailed observing parameters are listed in Table 2.

The spectra of well separated group galaxies were reduced using standard IRAF<sup>6</sup> processing tasks. Wavelength solutions were derived from a fit to sky lines on both sides of each spectrum, and independently confirmed with arc lamp spectra taken immediately before and after the science exposures. The agreement between the two solutions was in all cases better than 1  $\text{\AA}$ . No attempt was made to flux-calibrate the spectra.

The primary lensing galaxy G1 is within one arcsecond of the four quasar images and almost 6 magnitudes fainter than their combined flux (Impey et al. 1996, Yee & Ellingson 1994). To remove the quasar light, it was thus necessary to subtract a scaled quasar spectrum from the spectrum of G1 and interpolate over the remaining residuals of two strong quasar emission lines (Ly  $\alpha$  at 5600  $\text{\AA}$  and C IV at 7200  $\text{\AA}$ ). The resulting galaxy spectrum is shown against the spectrum of the quasar in Fig. 3. The quasar spectrum in this figure represents the sum of unresolved image A, B, and C fluxes.

We are unable to confirm the detection of weak [OII] and [OIII] emission lines in the spectrum of G1 that lead Hammer et al. (1995) to the conclusion that the lensing galaxy redshift is 0.647. Instead, we find a break in the continuum at 5300  $\text{\AA}$  and two absorption

---

<sup>6</sup>IRAF is distributed by the National Optical Astronomy Observatories, which are operated by the Association of Universities for Research in Astronomy, Inc., under cooperative agreement with the National Science Foundation.

lines blueward of the break that are well fitted by Ca H and K lines at  $z = 0.3374$ . Detection of the Na D line at  $7882 \text{ \AA}$  (top panel of Fig. 4) provides further confirmation of this redshift.

Accurate redshifts for galaxies G2–G6 were determined by cross-correlating their spectra with the templates of G and K giants published by Jones (1996) on the AAS CD-ROM 7 (Leitherer et al. 1997). The results of the cross-correlation analysis are summarized in Table 1. The errors listed in the table were calculated from the width of the cross-correlation peak (Tonry & Davis 1979) and an estimate of the systematic error in wavelength calibration. The spectra of five lensing galaxies are shown in Fig. 4. Major absorption features are marked in these spectra with vertical dotted lines. A closer inspection of the figure reveals a significant redshift difference ( $\Delta z = 0.005$ ) between G3, the brightest group galaxy, and the rest of the lensing group. Galaxy G3 is thus a large contributor to the high velocity dispersion of the group (see Table 3).

### 3. A Comparison Between the PG 1115+080 and the B 1422+231 Lensing Groups

The close proximity of galaxies G1–G6 in redshift and angular coordinates on the sky strongly suggests that they are members of a gravitationally bound compact group of galaxies. The rest-frame line-of-sight velocity dispersion of this group, estimated with  $\sigma_v = c\sigma_z/(1+z)$ , is  $550 \pm 50 \text{ km s}^{-1}$ . The median projected separation of group galaxies is  $35 h^{-1} \text{ kpc}$ , assuming  $\Omega = 1$ . At lower redshifts similar groups have been found by Hickson (1982) and studied in detail by Hickson et al. (1992). While the lensing group in the B 1422+231 system has a higher velocity dispersion than is typical of Hickson’s compact groups (HCGs), it is still within the range of Hickson’s sample. As we mentioned above, most of the velocity dispersion is contributed by the brightest group galaxy G3, whose rest-frame velocity is  $\sim 1100 \text{ km s}^{-1}$  higher than the median velocity of the group. This galaxy would be excluded by Hickson et al. (1992) from the sample of accordant members, which must have velocities within  $1000 \text{ km s}^{-1}$  of the group median. Excluding G3, the rest-frame velocity dispersion of the group would be only  $240 \pm 60 \text{ km s}^{-1}$ . However, because of its magnitude and central location within the group we retain G3 in the subsequent analysis.

There are at least three other QSO gravitational lens systems where the primary lens is surrounded by a group or a cluster: the double quasar Q 0957+561 (Walsh, Carswell, & Weymann 1979), the quadruple quasar PG 1115+080 (Weymann et al. 1980), and the recently discovered radio quad MG 0751+2716 (Lehár et al. 1997). In the largest-separation

confirmed lens system, Q 0957+561, the primary lens is positioned near the center of a medium-rich cluster with the velocity dispersion of  $715 \pm 130 \text{ km s}^{-1}$  (Angonin-Willaime, Soucail, & Vanderriest 1994). Both PG 1115+080 (Kundić et al. 1997) and MG 0751+2716 are lensed by compact groups of galaxies, although the redshifts of the MG 0751+2716 group galaxies are not yet available.

In Table 3 we compare properties of the two lensing groups that have been spectroscopically investigated at Keck: PG 1115+080 and B 1422+231. Both systems are similarly compact, but the velocity dispersion is much higher in B 1422+231 as a result of the large velocity difference between G3 and the rest of the group. Assuming that these lensing groups are self-gravitating, their masses can be estimated using the virial theorem (e.g. Heisler, Tremaine, & Bahcall 1985):

$$M = \frac{3\pi N}{2G} \frac{\sum_i v_i^2}{\sum_{i<j} 1/R_{\perp,ij}} \quad , \quad (1)$$

where  $v_i$  is the line-of-sight velocity of the  $i$ th galaxy relative to the centroid of the group, and  $R_{\perp,ij}$  is the projected separation of galaxies  $i$  and  $j$ . The virial estimates, as well as the light-weighted group centroids, are listed in Table 3. These values should be treated with caution, because of the small number of galaxies used to derive them. The assumptions inherent in the virial mass estimate (Eq. 1) and its accuracy in reproducing the masses of simulated groups are discussed by Heisler et al. (1985). These authors find that 75% of mass estimates lie within  $10^{0.25}$  of the correct value for groups with 5 members.

Frequent occurrence of groups and clusters near the primary lens is an important clue for statistical studies of gravitational lensing. Keeton, Kochanek, & Seljak (1996, hereafter KKS96) have convincingly shown that external shear is a more fundamental parameter for the lensing models than the radial distribution of mass in the primary lens. External sources of shear thus warrant careful observational scrutiny.

#### 4. Models

Shortly after discovery of B 1422+231, lens models of this system were constructed by Hogg & Blandford (1994, hereafter HB94) and by Kormann, Schneider, & Bartelmann (1994). It was realized by both groups that a substantial ellipticity in the potential is required to successfully reproduce the observed morphology of the system. However, the two sets of models disagree on the relative importance of external shear and internal ellipticity in breaking the circular symmetry of the lens potential. HB94 rely on strong external shear from two nearby bright galaxies, G2 and G3, while Kormann et al. make G1

highly elliptical. Subsequent *HST* observations of the lens (Impey et al. 1996) showed that its optical axis ratio  $a/b = 1.37 \pm 0.14$  is smaller than the ratio predicted by the Kormann et al. (1994) models,  $1.68 < a/b < 2.86$ . The observations can only be reconciled with the models if the dark matter distribution in the lens is significantly flatter than its optical isophotes.

More recently, KKS96 modeled B 1422+231 as part of their investigation of shear and ellipticity in gravitational lenses. A new observational input for these models was a precise position of the primary lens G1 provided by the *HST* imaging (Impey et al. 1996). KKS96 distinguish between two classes of models: single-shear and multiple-shear. Single-shear models feature only one source of ellipticity which is provided either by the primary lens or by an external shear field. In the two-shear models, there are two independent sources of ellipticity with major axes that are generally misaligned. Based on previous work (Kochanek 1991, Wambsganss & Paczyński 1994) and their own models, KKS96 argue that adding additional parameters to the radial distribution of a model generally does little to improve the fit. On the other hand, KKS96 show that including additional sources of shear often results in dramatic improvements. Unfortunately, this is not true for B 1422+231. The  $\chi^2$  of the one-shear model, in which the primary lens is modeled as a singular isothermal sphere perturbed by a quadrupole shear potential, is 40.3 for 6 degrees of freedom and 9 parameters. The corresponding two-shear model, consisting of a singular isothermal ellipsoid in an external shear field, has a  $\chi^2$  of 33.7 and 4 degrees of freedom (KKS96). The justification of adding new parameters to the model can be assessed with a standard F-test (e.g. Lupton 1993). According to this test, the probability of  $\chi^2$  decreasing from 40.3 to 33.7 when two *arbitrary* parameters are added to the model is 76%, suggesting that the second shear does not significantly reduce the  $\chi^2$ . Normally, the extra parameters would be accepted only if the F-test probability were smaller than 5%. Another reason to doubt the importance of the second shear term is the alignment of the two axes in the two-shear model: the angle between them is only  $4^\circ$  (KKS96). We are left with the conclusion that the best current model of the system consists of a singular isothermal sphere in the external shear field of the group, which is essentially the original HB94 model.

There are, however, two potential problems with the HB94 model: it requires large external shear from a massive perturber, and it fails to reproduce the flux ratio of images A and B at radio wavelengths. We consider these two problems in turn.

In the previous section, we estimated the lensing group mass using the virial theorem. We can divide this value with the combined  $K_s$  luminosity of group members, and compare the resulting near-infrared mass-to-light ratio of the lensing group with optical ratios of local groups. The total near-infrared luminosity of the lensing group galaxies, corrected by

–0.3 mag to account for the light outside of the 3'' aperture, is  $K_s = 14.9$ . At the redshift of  $z = 0.338$ , this corresponds to an absolute magnitude of  $M_{K_s} = -25.5 + 5 \log h$ , where  $H_0 \equiv 100 h \text{ km s}^{-1} \text{ Mpc}^{-1}$  and  $(\Omega, \Lambda) = (1, 0)$ . We applied a  $K$ -correction of –0.2 mag (Poggianti 1997) and neglected the evolutionary corrections and the difference between the  $K_s$  and  $K$  bands. Using the absolute magnitude of the Sun,  $M_{K_\odot} = +3.4$  (Allen 1973), we find that the near-infrared mass-to-light ratio of the group is  $40h$  in solar units. In a large sample of nearby groups Ramella et al. (1997) find that their blue mass-to-light ratios range between  $160h$  and  $330h$ . Taking into account that the mass-to-light ratio of an old stellar population is 6-8 times higher in blue than it is in  $K$  (Worthey 1994), we conclude that the B 1422+231 lensing group fits well within the Ramella et al. sample.

For the purpose of lens modeling, we can directly use the measured velocity dispersion of the group, but we have to make certain assumptions about the mass profile. If we model the group as a singular isothermal sphere, its velocity dispersion of  $550 \text{ km s}^{-1}$  acting at an angular distance of  $\sim 14$  arcsec will produce the dimensionless shear of  $\gamma = 0.23$  at the position of the lens. This shear is consistent with the value expected in the HB94 model and the related one-shear KKS96 model. It is also worth noting that group galaxies G2–G6 are so close to the line of sight to the QSO that they undoubtedly contribute to the convergence (dimensionless surface mass density) as well as the shear. If the lensing group has singular isothermal sphere profile, the convergence  $\kappa$  is equal to the shear  $\gamma$ . A uniform convergence term in the model does not affect the observed image positions and relative fluxes; however, it will affect the inferred distance to the lens when the time delays are measured (Falco, Gorenstein, & Shapiro 1985).

We have accounted for the presence of a massive perturber, but the fact that the HB94 model fails to reproduce the radio flux ratio of images A and B remains a serious problem. In the refined model of HB94 the relative magnification of these two images is 0.77, many standard deviations away from the radio measurement of  $0.98 \pm 0.02$  (Patnaik et al. 1992a). However, optical and near-infrared measurements have consistently produced lower flux ratios clustering around 0.8 (Lawrence et al. 1992, Remy et al. 1993, Yee & Ellingson 1994, Hammer et al. 1995, Akujor et al. 1996, Impey et al. 1996, Yee & Bechtold 1996). It is difficult to explain the difference between the radio and the optical as a result of absorption along the line of sight to the quasar because the flux ratio is nearly identical in all bands between  $U$  and  $K_s$ . It is also unlikely that it can be explained by microlensing since the ratio has not changed over at least a year (Yee & Bechtold 1996) and even longer if data taken by different observers are included. Regardless of which ratio represents the true relative magnification of the two images, it is important that we explain the observed discrepancy, as it may have profound consequences for models of other gravitational lens systems.



## 5. Discussion

Based on Keck spectroscopy of the gravitational lens system B 1422+231, we conclude that the primary lens and four nearby objects belong to a compact group of galaxies at  $z_d = 0.338$ . The virial mass of this group, inferred from its median projected radius of  $35 h^{-1}$  kpc and its velocity dispersion of  $\sim 550 \text{ km s}^{-1}$ , amounts to  $1.4 \times 10^{13} h^{-1} M_\odot$ . This concentration of mass, located some  $14''$  from the quasar images, is sufficient to produce the observed image configuration in a simple lens model consisting of a singular isothermal sphere in a strong external shear field. The same model successfully accounts for the optical and near-infrared flux ratios of the images, although it remains inconsistent with the relative magnification of images A and B in radio. An accurate lens model for this system is of great importance because photometric monitoring shows the source to be intrinsically variable on the timescales comparable to the predicted time delay between the triplet ABC and image D (Hjorth et al. 1996, Yee & Bechtold 1996, Turner et al. 1997). Using the lens redshift of  $z_d = 0.338$ , the HB94 model predicts this time delay to be about  $15 h^{-1}$  days. The delays between images A, B and C are all smaller than a day – too short to measure at optical and radio wavelengths.

By trimming down model space and reducing the uncertainty in predicted time delays, the observations presented here improve the chances of using this system to measure the Hubble constant. Together with the spectroscopic observations of PG 1115+080 (Kundić et al. 1997), they also suggest that a number of gravitational lens systems are influenced by significant external shear. The external shear provided by galaxies associated with the primary lens naturally explains why many lens models require potentials that are more elliptical than the images of the primary lensing galaxy would suggest. External shear could also be responsible for the large number of quadruple lenses relative to the doubles (King et al. 1996). A spectroscopic survey of the fields around other gravitational lenses would thus provide valuable observational input for estimates of external shear in these systems.

We are grateful to the W. M. Keck Foundation for the vision to fund the construction of the W. M. Keck Observatory. We thank Charles Lawrence, Keith Matthews, Gerry Neugebauer and Tom Soifer for making their unpublished near-infrared data available. We benefited from helpful conversations with Sangeeta Malhotra and Michael Pahre. Financial support was provided by NSF grants AST 92–23370 and AST 95–29170, and by NASA grant NAG 5-3834. This research made use of NASA’s Astrophysics Data System Abstract Service.

## REFERENCES

- Akujor, C. E., Patnaik, A. R., Smoker, J. V., & Garrington, S. T. 1996, in *Astrophysical Applications of Gravitational Lensing*, ed. C. S. Kochanek, & J. N. Hewitt (Dodrecht: Kluwer), 335
- Allen, C. W. 1973, *Astrophysical Quantities*, 3rd ed. (London: Athlone Press), p. 162
- Angonin-Willaime, M.-C., Soucail, G., & Vanderriest, C. 1994, *A&A*, 291, 411
- Bechtold, J., & Yee, H. K. C. 1995, *AJ*, 110, 1984
- Blandford, R. D., & Kundić, T. 1997, in *The Extragalactic Distance Scale*, ed. M. Livio, M. Donahue, & N. Panagia (Cambridge: Cambridge University Press), in press
- Casali, M. M., & Hawarden, T. G. 1992, *JCMT-UKIRT Newsletter*, 3, 33
- Falco, E. E., Gorenstein, M. V., & Shapiro, I. I. 1985, *ApJ*, 289, L1
- Hammer, F., Rigaut, F., Angonin-Willaime, M.-C., & Vanderriest, C., 1995, *A&A*, 298, 737
- Heisler, J., Tremaine, S., & Bahcall, J. N. 1985, *ApJ*, 298, 8
- Hickson, P. 1982, *ApJ*, 255, 382
- Hickson, P., Mendes de Oliveira, C., Huchra, J. P., & Palumbo, G. G. C. 1992, *ApJ*, 399, 353
- Hjorth, J., Jaunsen, A. O., Patnaik, A. R., & Kneib, J.-P. 1996, in *Astrophysical Applications of Gravitational Lensing*, ed. C. S. Kochanek, & J. N. Hewitt (Dodrecht: Kluwer), 343
- Hogg, D. W., & Blandford, R. D. 1994, *MNRAS*, 268, 889 (HB94)
- Impey, C. D., Foltz, C. B., Petry, C. E., Browne, I. A. W., & Patnaik, A. R. 1996, *ApJ*, 462, L53
- Jones, L. 1996, Ph.D. thesis, University of North Carolina at Chapel Hill
- Keeton, C. R., Kochanek, C. S., & Seljak, U. 1996, preprint, astro-ph/9610163 (KKS96)
- King, L. J., Browne, I. W. A., Wilkinson, P. N., & Patnaik, A. 1996, in *Astrophysical Applications of Gravitational Lensing*, ed. C. S. Kochanek, & J. N. Hewitt (Dodrecht: Kluwer), 191
- Kochanek, C. S. 1991, *ApJ*, 373, 354
- Kormann, R., Schneider, P., & Bartelmann, M. 1994, *A&A*, 286, 357
- Kundić, T. et al. 1996, preprint, astro-ph/9610162
- Kundić, T., Cohen, J. G., Blandford, R. D., & Lubin, L. M. 1997, preprint, astro-ph/9704109

- Lawrence, C. R., Neugebauer, G., Weir, N., Matthews, K., & Patnaik, A. R. 1992, MNRAS, 259, 5P
- Lehár J. et al. 1997, preprint, astro-ph/9702191
- Leitherer, C. et al. 1997, PASP, 108, 996
- Lupton, R. 1993, *Statistics in Theory and Practice* (Princeton: Princeton University Press), p. 100
- Matthews, K., & Soifer, B. T. 1994, in *Infrared Astronomy with Arrays*, ed. I. McLean (Dodrecht: Kluwer), 239
- Oke, J. B., et al. 1995, PASP, 107, 375
- Patnaik, A. R., Browne, I. W. A., Walsh, D., Chaffee, F. H., & Foltz, C. B. 1992, MNRAS, 259, 1P
- Patnaik, A. R., Browne, I. W. A., Wilkinson, P. N., & Wrobel, J. M. 1992, MNRAS, 254, 655
- Patnaik, A. R. 1994, in *Gravitational Lenses in the Universe*, ed. J. Surdej, D. Fraipont-Caro, E. Gosset, S. Refsdal, & M. Remy (Liège, Belgium: Université de Liège, Institut d’Astrophysique), 311
- Poggianti, B. M. 1997, A&AS, 122, 399
- Ramella, M., Pisani, A., & Geller, M. J. 1997, AJ, 113, 483
- Refsdal, S. 1964, MNRAS, 128, 307
- Remy, M., Surdej, J., Smette, A., & Claeskens, J.-F. 1993, A&A, 278, L19
- Schechter, P. L. et al. 1997, ApJ, 475, L85
- Tonry, J., & Davis, M. 1979, AJ, 84, 1511
- Turner, E. L. et al. 1997, in preparation
- Walsh, D., Carswell, R. F., & Weymann, R. J. 1979, Nature, 279, 381
- Wambsganss, J., & Paczyński, B. 1994, AJ, 108, 1156
- Weymann, R. J., Latham, D., Angel, J. R. P., Green, R. F., Liebert, J. W., Turnshek, D. A., Turnshek, D. E., & Tyson, J. A. 1980, Nature, 285, 641
- Worthey 1994, ApJS, 95, 107
- Yee, H. K. C., & Ellingson, E. 1994, AJ, 107, 28
- Yee, H. K. C., & Bechtold, J. 1996, AJ, 111, 1007

Table 1. Lensing Galaxy Positions, Magnitudes and Redshifts

Galaxy	$-\Delta\alpha$ (")	$\Delta\delta$ (")	$V^1$	$R$	$i^1$	$J$	$H$	$K_s$	Redshift
G1	−0.7	−0.6	21.5 <sup>2</sup>	$r = 21.8^3$	...	...	...	...	$0.3374 \pm 0.0005$
G2	−9.4	−4.9	20.4	19.9	19.1	17.1	17.9	16.4	$0.3379 \pm 0.0005$
G3	−3.9	−7.2	20.0	19.6	18.8	16.7	17.5	16.0	$0.3427 \pm 0.0005$
G4	−7.5	−10.4	21.6	21.0	20.5	18.4	19.0	17.6	$0.3366 \pm 0.0005$
G5	−17.4	−28.8	20.3	20.0	19.4	...	...	...	$0.3384 \pm 0.0005$
G6	4.4	−7.4	...	22.2	...	20.2	20.3	19.9	$0.3357 \pm 0.0005$
G7	16.7	−12.0	...	23.0	...	18.9	...	18.4	...
G8	−2.1	12.9	...	22.4	...	20.2	20.7	20.0	$0.2355 \pm 0.0005$
G9	25.5	35.0	...	21.7	...	...	...	...	$0.4650 \pm 0.0005$
G10	16.6	−41.5	...	22.2	...	...	...	...	$0.4055 \pm 0.0005$
S1	6.9	−15.9	18.1	17.4	17.1	15.7	...	15.6	...

Note. — (1)  $V$  and  $i$  magnitudes are taken from Remy et al. (1993); (2)  $V$  magnitude of G1 is taken from Impey et al. (1996); (3) Gunn  $r$  magnitude of G1 is adopted from Yee & Ellingson (1994).

Table 2. Observing Parameters

Exposure Number	Object	UT Date	UT Time	Airmass	PA (°E of N)	Exposure Time (s)	Grating lines/mm	Wavelength Range (Å)
1	G2, G3	1995 Jul 30	05:55	1.09	69	1800	300	3960-8970
2	G2, G3	1995 Jul 30	06:27	1.16	69	1200	300	3960-8970
3	QSO, G1, G9	1995 Jul 31	06:14	1.14	315	1000	300	3960-8970
4	QSO, G1, G9	1995 Jul 31	06:32	1.19	315	1000	300	3960-8970
5	QSO, G1	1995 Jul 31	07:07	1.32	315	1000	300	3960-8970
6	G4, G5	1997 Mar 2	14:17	1.00	332	1200	600	4770-7310
7	G5	1997 Mar 2	14:52	1.02	327	1200	600	4770-7310
8	G6, G8, G10	1997 Jun 2	09:12	1.04	18	1600	600	4260-6780
9	G6, G8, G10	1997 Jun 2	09:41	1.09	18	1000	600	4260-6780
10	G6, G8, G10	1997 Jun 2	09:59	1.13	18	1800	600	5640-8190

Table 3. Lensing Group Properties: PG 1115+080 and B 1422+231

Gravitational Lens System	PG 1115+080	B 1422+231
Number of Galaxies	4	6
Group Redshift	0.311	0.338
Velocity Dispersion (km s <sup>-1</sup> )	270 ± 70	550 ± 50
Median Projected Galaxy Separation ( $h^{-1}$ kpc)	35	35
Virial Mass ( $h^{-1} M_{\odot}$ )	$4.6 \times 10^{12}$	$1.4 \times 10^{13}$
Group Centroid ( $d, \theta$ ) <sup>1</sup>	(17", -121°)	(14", 146°)

Note. — (1) The luminosity-weighted center of the group is specified relative to image C in PG 1115+080 and relative to image B in B 1422+231. The distance of the centroid is quoted in arcseconds and its position angle is measured north through east.

Fig. 1.—  $R$  band image of the  $2' \times 2'$  field surrounding the gravitational lens system B 1422+231. North is up and east is to the left. The central bright object contains four unresolved quasar images and the primary lens galaxy G1. The remaining lensing group galaxies G2–G6 are located southeast of the quasar. G7 has not been studied spectroscopically, while G8, G9 and G10 are emission line galaxies with redshifts 0.2355, 0.4650 and 0.4055. Positional reference star S1 is also marked in the figure.

Fig. 2.—  $K_s$  band image of B 1422+231 in  $0.7''$  seeing. The field is  $38.4''$  on the side with north up and east to the left. Object names are same as in Fig. 1. The location of the luminosity-weighted centroid of the group is roughly coincident with G4.

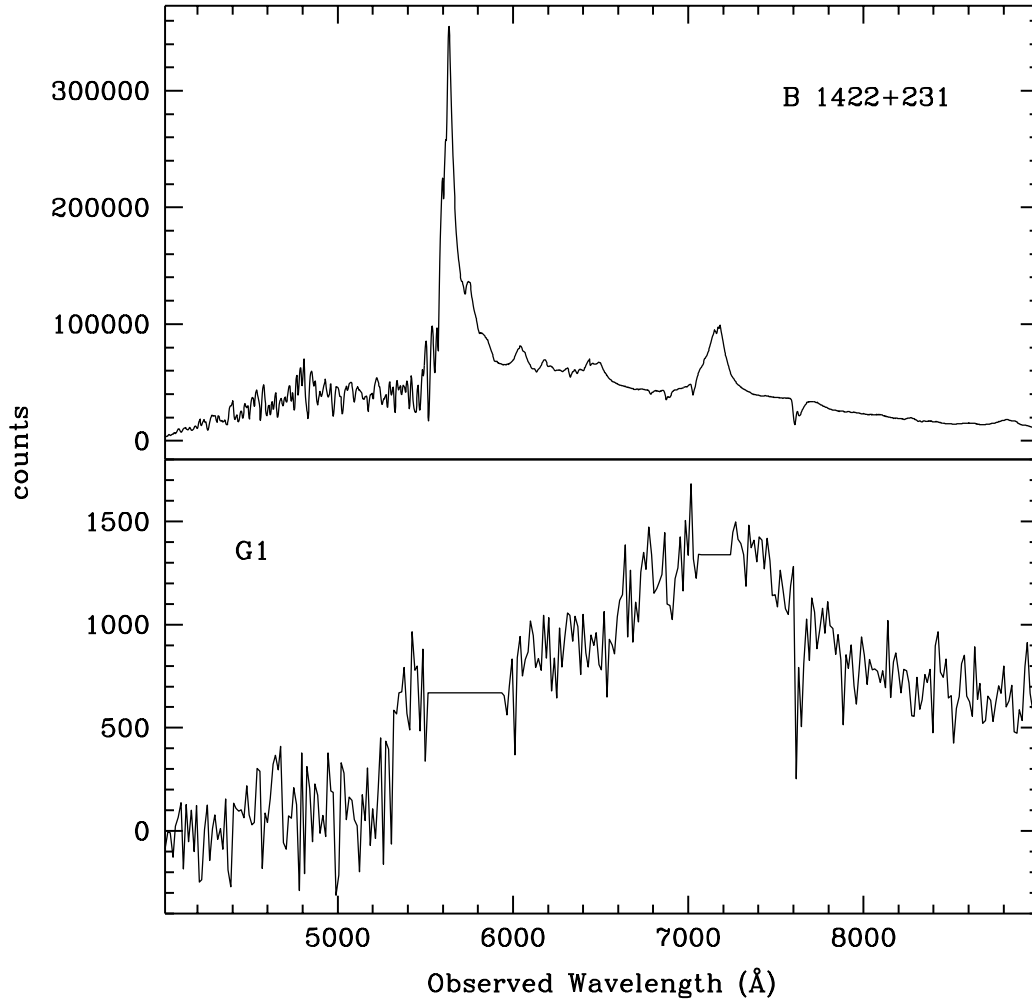


Fig. 3.— Composite spectrum of B 1422+231 (*top*), and the primary lens galaxy G1 (*bottom*). We have interpolated over the residuals of broad quasar emission lines in the G1 spectrum and smoothed the spectrum to  $15\text{\AA}$  resolution. The redshift of G1 was determined from the Ca H and K lines blueward of the  $4000\text{\AA}$  break (observed at  $5350\text{\AA}$ ) and the Na D line observed at  $7882\text{\AA}$ .

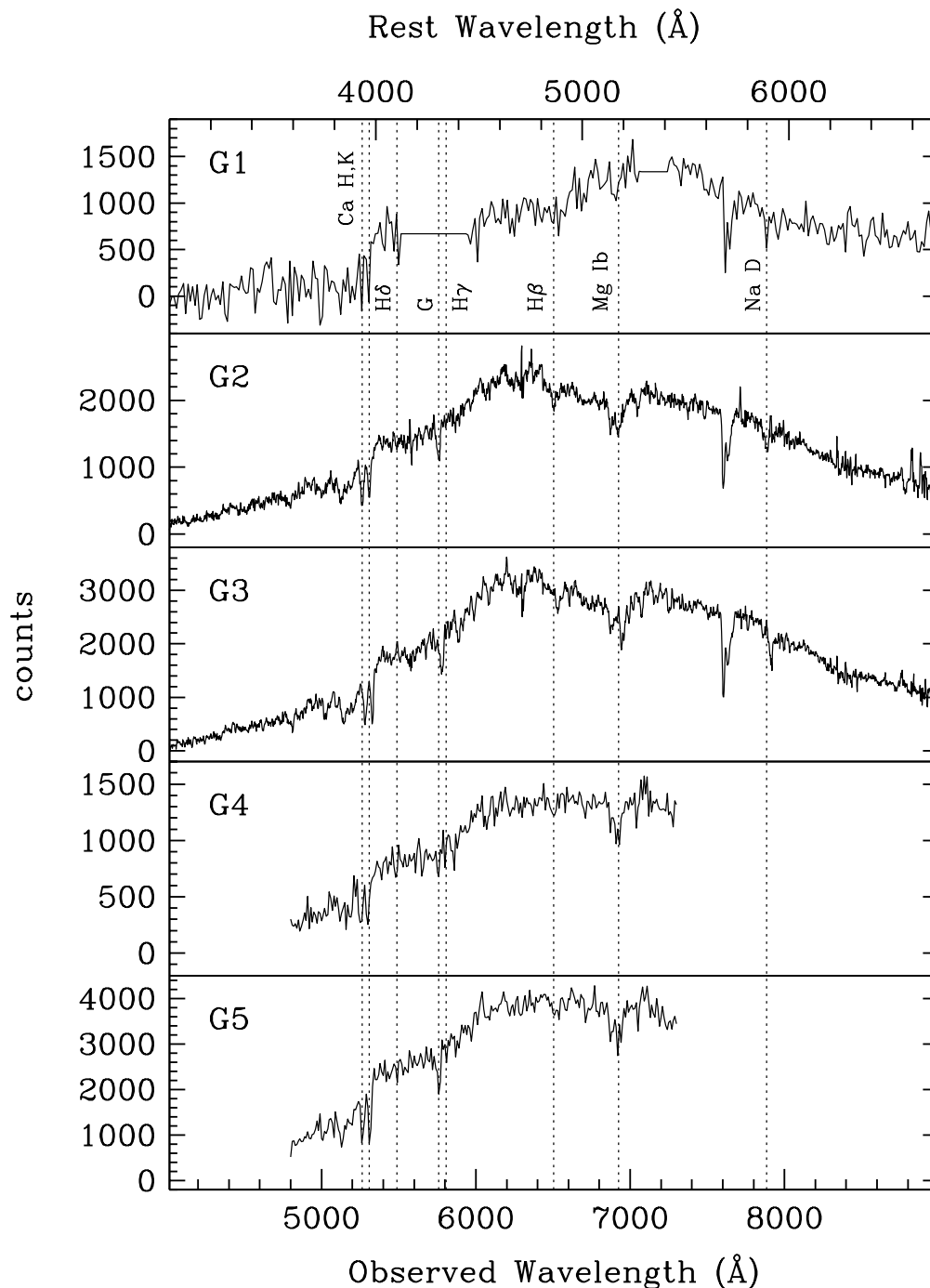


Fig. 4.— The spectra of the primary lens G1 and group galaxies G2, G3, G4 and G5 (*top to bottom*). In order to suppress noise, G1 spectrum is binned to  $15\text{\AA}$  resolution, while G4 and G5 spectra are binned to  $10\text{\AA}$  resolution. High signal-to-noise G2 and G3 spectra are shown at instrumental resolution. Strong spectral features are identified with dotted lines assuming the group redshift of  $z = 0.338$ . The same redshift is used for the rest wavelength scale on the top of the figure. Note the redshift difference between G3 (the brightest group member) and the other four galaxies.



This figure "figure1.jpg" is available in "jpg" format from:

<http://arxiv.org/ps/astro-ph/9706169v1>

This figure "figure2.jpg" is available in "jpg" format from:

<http://arxiv.org/ps/astro-ph/9706169v1>